

REPORT DOCUMENTATION PAGE

Form Approved
OMB No. 0704-0188

maintaining the data needed, and completing and reviewing this collection of information. Send comments regarding this burden estimate or any other aspect of this collection of information, including suggestions for reducing this burden to Department of Defense, Washington Headquarters Services, Directorate for Information Operations and Reports (0704-0188), 1215 Jefferson Davis Highway, Suite 1204, Arlington, VA 22202-4302. Respondents should be aware that notwithstanding any other provision of law, no person shall be subject to any penalty for failing to comply with a collection of information if it does not display a currently valid OMB control number. PLEASE DO NOT RETURN YOUR FORM TO THE ABOVE ADDRESS.

1. REPORT DATE (DD-MM-YYYY) 29-08-2007	2. REPORT TYPE Final Performance Report	3. DATES COVERED (From - To) 1 Dec 2003 - 31 May 2007
--	---	---

MEASUREMENT OF ATMOSPHERIC PRESSURE AIR PLASMA VIA PULSED ELECTRON BEAM AND SUSTAINING ELECTRIC FIELD

5a. CONTRACT NUMBER
5b. GRANT NUMBER FA9550-04-1-0015
5c. PROGRAM ELEMENT NUMBER

6. AUTHOR(S)
Robert J Vidmar and Kenneth R Stalder

5d. PROJECT NUMBER
5e. TASK NUMBER
5f. WORK UNIT NUMBER

7. PERFORMING ORGANIZATION NAME(S) AND ADDRESS(ES)

University of Nevada, Reno
Sponsored Projects, Mail Stop 325
1664 N Virginia Street
Reno, NV 89557-0240

8. PERFORMING ORGANIZATION REPORT NUMBER

9. SPONSORING / MONITORING AGENCY NAME(S) AND ADDRESS(ES)

AF Office of Scientific Research
4015 Wilson Blvd, Room 713
Arlington, VA 22203-1954

10. SPONSOR/MONITOR'S ACRONYM(S)
AFOSR/NE

Dr Robert Barker/NE

11. SPONSOR/MONITOR'S REPORT

AFRL-SR-AR-TR-07-0338

12. DISTRIBUTION / AVAILABILITY STATEMENT

UNLIMITED *Distribution Statement A: unlimited*

13. SUPPLEMENTARY NOTES

14. ABSTRACT

An apparatus to study the generation of plasma in air was designed, fabricated, and assembled. A 400-liter test cell was developed to study plasma in air which has a pressure that can be varied from standard atmospheric pressure at sea level to 1 mTorr at 300,000 ft. Plasma is generated by impact ionization of air due to bombardment by a 100-keV electron beam. Microwave diagnostics quantify electron number density and optical diagnostics quantify ozone production. A particle in cell plasma code (MAGIC) and an air-chemistry code are used to quantify beam propagation through an electron-beam transmission window into air and the volumetric ionization rate within the test cell. Sensors were developed to monitor beam current incident on a transmission window and the resulting plasma formed in air on the transmission side of the window. Diagnostics from multiple sensors are acquired simultaneously for studies of power required to generate and maintain plasma in air on the timescale of 1 ms.

15. SUBJECT TERMS

Air Chemistry, Air Plasma, MAGIC Modeling, Plasma, Power, Test-Cell

16. SECURITY CLASSIFICATION OF:			UNCLASSIFIED	17. LIMITATION OF ABSTRACT	18. NUMBER OF PAGES 25	19a. NAME OF RESPONSIBLE PERSON Robert J Vidmar
a. REPORT UNCLASSIFIED	b. ABSTRACT UNCLASSIFIED	c. THIS PAGE UNCLASSIFIED	UNCLASSIFIED UNLIMITED	19b. TELEPHONE NUMBER (include area code) 775 682-9742		

**MEASUREMENT OF ATMOSPHERIC PRESSURE AIR PLASMA VIA
PULSED ELECTRON BEAM AND SUSTAINING ELECTRIC FIELD**

By: ROBERT J VIDMAR

Prepared for:

AIR FORCE OFFICE OF SCIENTIFIC RESEARCH
4015 WILSON BOULEVARD, ROOM 713
ARLINGTON, VA 22203-1954

CONTRACT NUMBER: FA9550-04-1-0015

Approved for Public Release: Unclassified with Distribution Unlimited

20070917134

University of Nevada, Reno
1664 North Virginia Street
Reno, Nevada 89557-0240 USA

ABSTRACT

An apparatus to study the generation of plasma in air was designed, fabricated, and assembled. A 400-liter test cell was developed to study plasma in air which has a pressure that can be varied from standard atmospheric pressure at sea level to 1 mTorr at 300,000 ft. Plasma is generated by impact ionization of air due to bombardment by a 100-keV electron beam. Microwave diagnostics quantify electron number density and optical diagnostics quantify ozone production. A particle in cell plasma code (MAGIC) and an air-chemistry code are used to quantify beam propagation through an electron-beam transmission window into air and the volumetric ionization rate within the test cell. Sensors were developed to monitor beam current incident on a transmission window and the resulting plasma formed in air on the transmission side of the window. Diagnostics from multiple sensors are acquired simultaneously for studies of power required to generate and maintain plasma in air on the timescale of 1 ms.

CONTENTS

ABSTRACT	ii
I INTRODUCTION	1
II TECHNICAL	2
A. Air Plasma Test Cell	2
B. Electron-Beam Source	3
C. Transmission Window	4
D. MAGIC Modeling	5
E. RF Diagnostics	6
F. Ozone Detection	7
G. Multichannel Simultaneous Data Acquisition	7
III RESULTS	8
A. Complete Facility	8
B. Multichannel Data Acquisition	8
IV PERSONNEL, INTERACTIONS, AND PUBLICATIONS	12
REFERENCES	14
APPENDIX	
MAGIC TEST CELL GEOMETRY	A-2
MAGIC DIAGNOSTIC DATA	A-3

FIGURES

1. Upper flange of test cell.	2
2. Main body of test cell.	6
3. Installed test cell with specifications.	9
4. High-voltage rack and electron gun mounted to upper flange of test cell.	11
5. Transmission window and current sensors.	12
6. Mesh sensor mounted in Teflon insulator connected to brass feedthrough.	13
7. Aluminum transmission window loaded with atmospheric pressure.	13
8. Mid plane ionization rate, beam current, and radial distribution.	13
9. RF horn mounting fixture detail.	13
10. Time domain S_{12} of internal reflections at 10 GHz with absorber.	14
11. White cell mounted in air-plasma test cell for ozone measurement.	
12. Hamamatsu H5783-03 mount and filter housing.	

TABLES

1. Multichannel diagnostics.	10
------------------------------	----

I INTRODUCTION

The overall goal of investigating the power required to generate and sustain electron-beam produced plasma in air was advanced with an apparatus designed to study power and air chemistry issues. The apparatus consists of an electron-beam source, a transmission window system, an air-plasma test cell, RF diagnostics, optical diagnostics, and a data acquisition system. The apparatus progressed from concept, specifications, component orders, assembly, testing, and refinement.

The overall investigation of electron-beam generated air plasma resulted in the development of an air plasma test cell integrate with an electron beam source, diagnostics, and an air-chemistry simulation code. This instrument and the associated controls and diagnostics provide an apparatus to quantify air-plasma generation in air with a pressure ranging from 1 mTorr to 760 Torr. At the start of this project there was an empty laboratory. An air-plasma test cell was designed, fabricated, and installed. An electron beam source was specified ordered and installed. To port the electron gun into the test cell a transmission window and beam current monitoring system was designed and installed. Beam propagation through the transmission window into air is modeled using MAGIC, a PIC plasma simulation code from ATK Technologies. An air-chemistry code is used to convert beam current estimates in the test cell to electron densities and air species concentrations. RF diagnostics and an ozone detection system were developed and installed.

Nonequilibrium plasma has been theoretically estimated by Vidmar (1990) to require less power to generate and sustain than a plasma in thermal equilibrium. The experimental work of Macheret *et al* (2001) for ambient air at 700 K, Adamovich (2001) for optically pumped CO/Ar/O₂ and CO/Ar/N₂ mixtures at 700 K, Yu *et al* (2002) for air at 2,000 K, and Stark and Schoenbach (2001) for air at 2,000 K consistently demonstrate that a nonequilibrium plasma requires less power for bulk gas temperature significantly above ambient. The electron beam air-plasma apparatus has the capability to generate a nonequilibrium plasma for which the bulk gas remains at ambient temperature.

The DoD has found air plasma applications ranging from coating of implants, plasma surgery, bio-decontamination, hydrodynamic flow control on aerodynamic surfaces, supersonic shock-wave mitigation, plasma assisted combustion in aircraft engines, RF effects, and agile plasma mirrors. These applications cover the range of altitudes from sea level to 300,000 ft with electron densities from 10¹⁰ to 10¹³ electrons/cm³. Electron beam plasma generation is the most efficient system known requiring an average expenditure of 34 eV per electron-ion pair. Preheating of air is unnecessary and air temperature for short pulses remains at the ambient air temperature. For large volumetric and airborne applications electron-beam ionization can fill large volumes and large angle scattering in air provides a means of filling irregular shapes and regions not directly exposed to the electron beam. The plasma generated is generally nonequilibrium where the bulk gas temperature remains near ambient and the electron temperature is many times larger.

II TECHNICAL APPROACH

A. Air Plasma Test Cell

The air-plasma test cell was designed to facilitate a wide range of diagnostics and accommodate 1mTorr to 760 Torr operation, as well as high vacuum to facilitate calibration of the electron gun source and leak detection. The drawings in Fig. 1 and 2 quantify the design which anticipated a number of ports of different diameters positioned on the midplane of the test cell. These ports are currently populated with equipment devoted to RF diagnostics, laser absorption spectroscopy, emission spectroscopy, ozone absorption spectroscopy, and mass spectroscopy. The installed test cell with annotated specifications appears in Fig 3.

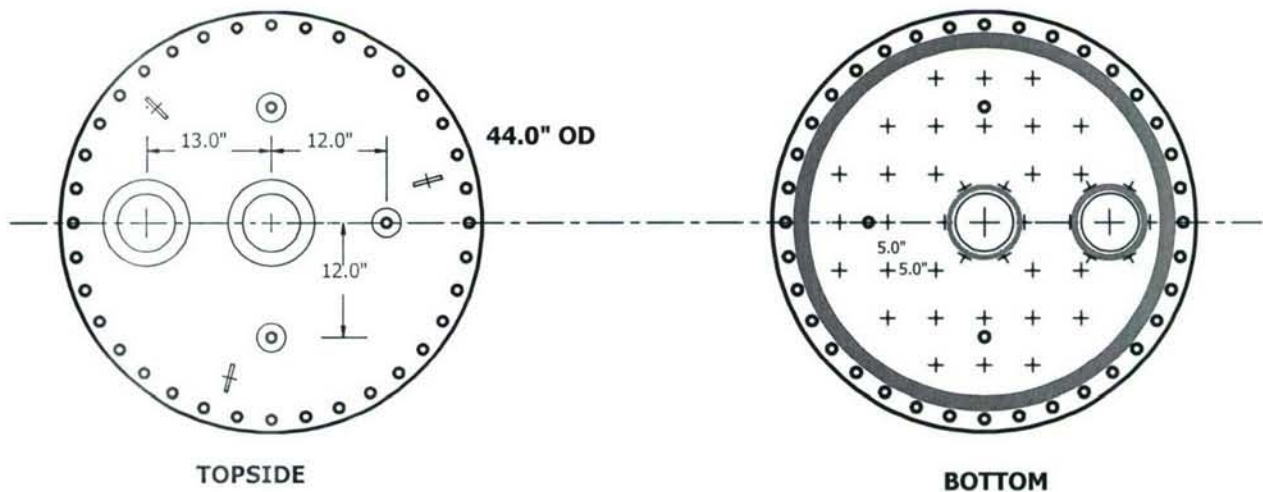


Figure 1. Upper flange of test cell.

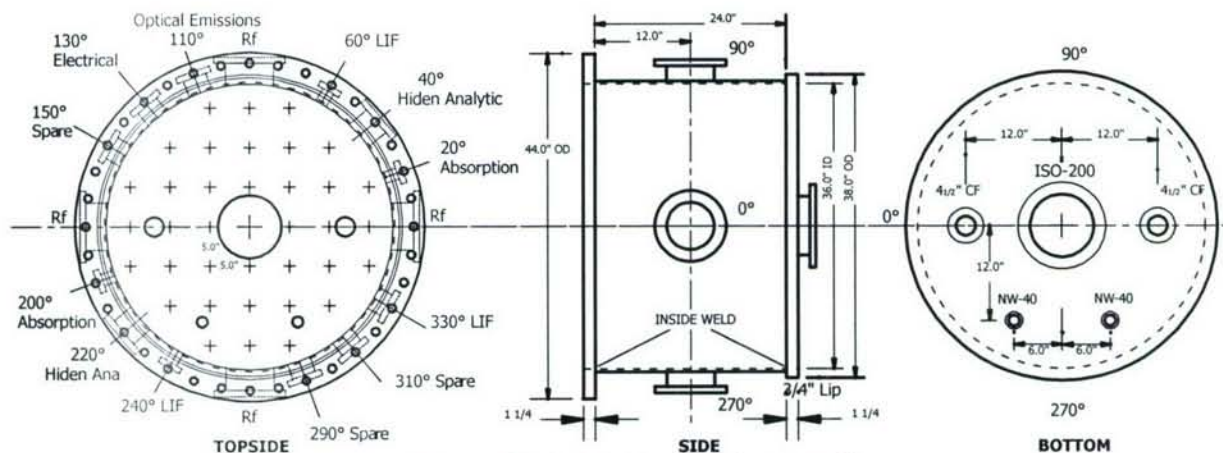


Figure 2. Main body of test cell.

The port specifications noted in Fig 2 have evolved since the fabrication of the test cell. RF diagnostics are between the ports at 0° and 180°, and a mass spectrometer is being attached to the port at 270°. The cell sits on a sturdy stand with vacuum pumps

INSIDE DIAMETER: 36", 91.44 cm
INSIDE HEIGHT: 24", 60.96 cm
VOLUME: 24,430 in³, 400.4 liter
SURFACE: 4,750 in², 3.065 m²

6" CF ELECTRON GUN PORTS
100 KV, 10 ma

PORTS ON CIRCUMFERENCE
 4 8" CF
 2 6" CF
 6 4 1/2" CF
 4 2 3/4" CF

4 1/2" CF SPARES

8" CF NIPPLE
RF DIAGNOSTICS

4 1/2" CF QUARTZ WINDOW



Figure 3. Installed test cell with specifications.

directly below. An I-beam and chain-hoist system were installed in the air-plasma laboratory to facilitate removal of the electron gun, lead shielding, and upper flange, which together exceeded 700 lbm.

B. Electron-Beam Source

3

An electron beam source was specified and procured from Kimball Physics of Wilton, NH. The unit in Fig. 4 is a custom design and has now become a product referred to as a EGH-8201 Electron Gun and EGPS-8201 power supply. The electron gun is operated at an energy of 100 kV with a maximum beam current in excess of 20 ma and arbitrary pulse generation with 100 ns rise/fall time. In normal operation the end of the electron gun is sealed off with a transmission window to keep the vacuum in the electron gun below 10^{-7} Torr. Initial operation of the electron gun had a high level of maintenance and repair as many components failed due to spurious current surges in the electron gun while performing high-voltage conditioning. A problem arose at 50 kV that necessitated return of a high voltage junction box to Kimball to replace a high-voltage isolation transformer and associated components. Approximately 100 lbm of lead shielding is used around the perimeter of the electron gun and so reduces the background radiation level to approximately twice background above the perimeter of the 44 in upper flange. One meter further away from the flange are operating consoles where the background radiation remains normal during operation.

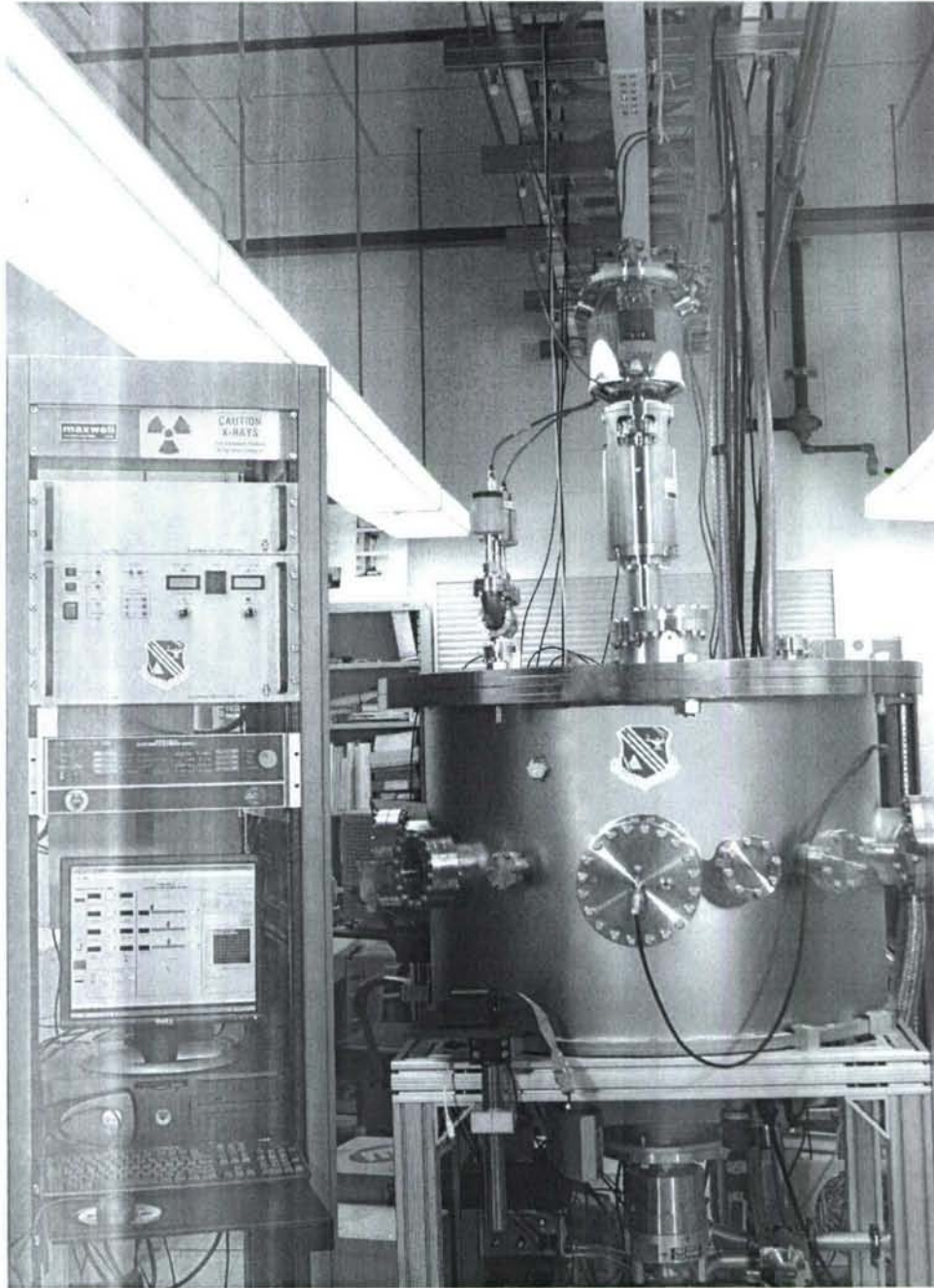


Figure 4. High-voltage rack and electron gun mounted to upper flange of test cell.

One major shortcoming of the EGH-8201 Electron Gun and EGPS-8201 power supply is the beam current monitoring design, which is for steady state operation. For microsecond and millisecond operation the Kimball current meters that monitor current flow from a high-voltage power supply do respond quickly enough. For short pulses the charge involved is a small fraction of the charge stored within the high-voltage cabling of the system. A solution for real-time current monitoring is addressed in the next section.

C. Transmission Window

The porting of an electron beam from the source through a transmission window is sketched in Fig. 5. The electron beam passes through a 60-mm aperture that defines the maximum beam diameter downstream. The beam then impinges on a nickel mesh with 98% transparency that is mounted in a Teflon insulator. Part of the beam is stopped by the mesh and so provided a signal that is proportional to the beam current. Most of the beam continues and passes through an aluminum honeycomb covered with a thin aluminum foil. The foil honeycomb and O-ring seals (not shown in Fig. 5) are compressed with an aluminum clamping ring with mounting bolts insulated from ground. The overall signal associated with the foil window consists of the current stopped by the foil and honeycomb plus the current associated with secondary electron generation on the foil and honeycomb and the shunt resistance from the foil surface to ground associated with the air plasma.

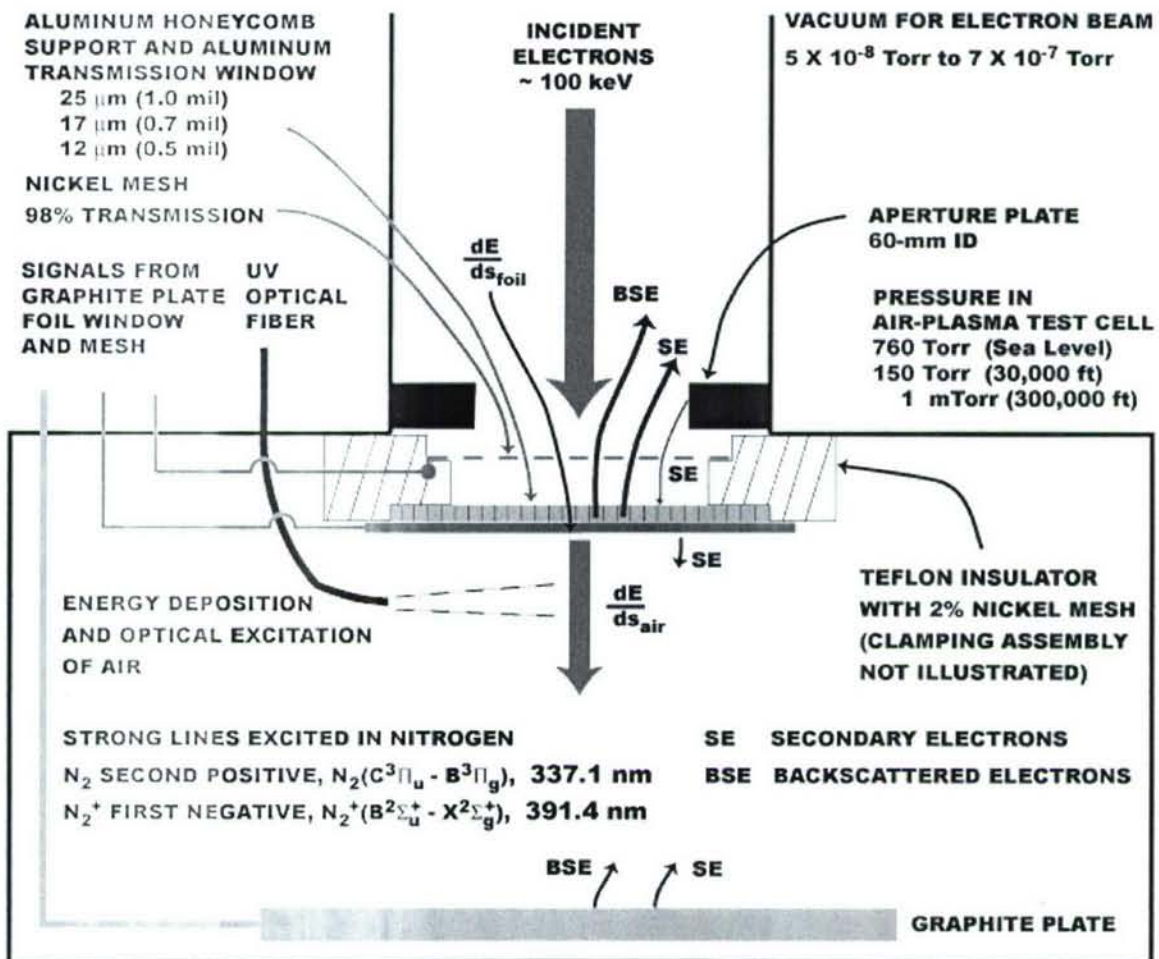


Figure 5. Transmission window and current sensors.

The 2-mil nickel is visible in Fig. 6 as well as the honeycomb structure on the opposite side of the Teflon insulator and the bottom side of an aluminum clamping ring.

The electrical connection for the mesh is made through the Teflon ring and sealed with the brass electrode visible in Fig. 6. This assembly is turned upside down and a transmission window foil is placed over the honeycomb and sealed with an O-ring between the Teflon and the foil.



Figure 6. Mesh sensor mounted in Teflon insulator connected to brass feedthrough.

The 1-mil aluminum transmission window foil made from Alloy 1100-O shown in Fig. 7 is held in place with an aluminum clamping ring which is bolted to the lower surface of the upper flange in Fig. 1 and 3. The electron gun is mounted on the opposite side of the upper flange and evacuated to a high vacuum for electron acceleration. The honeycomb provides mechanical support against the loading due to atmospheric pressure. The mechanical design has been tested with atmospheric pressure loading for hundreds of hours without any sign of honeycomb failure.

Transmission window failures have occurred due to overheating the foil which results in a pinhole leak. Aluminum foils of alloy 1100-O in thicknesses of 0.75 mil and 0.50 mil have been tried but stress related pinholes appeared several days after evacuation. These failures suggest that a material with high tensile strength would survive. Aluminum alloys 2024-T3, T4, T351, and T361 and 5052-H32, H34, H36, and H38 have tensile strengths between 5 and 10 times that of alloy 1100-O. Obtaining higher strength alloy foils is difficult.

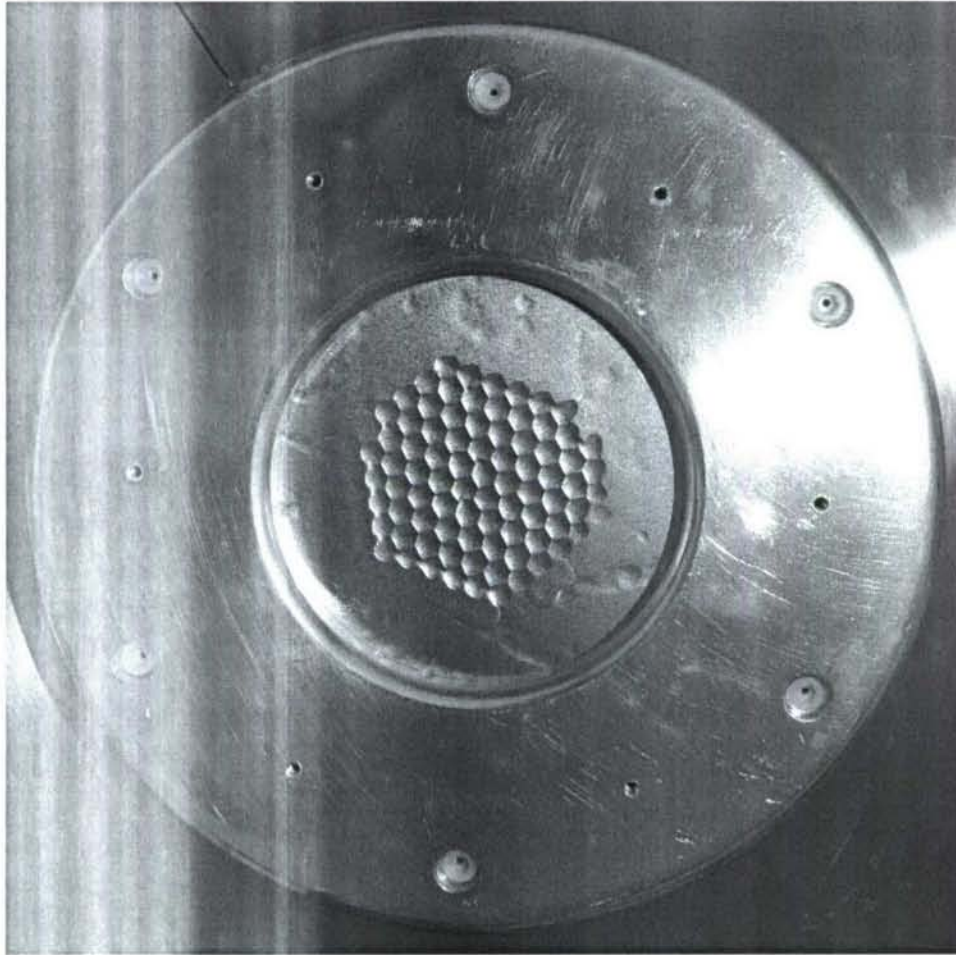


Figure 7. Aluminum transmission window loaded with atmospheric pressure.

In operation the system is calibrated with the honeycomb and foil removed and a graphite plate with a fluorescent coating placed on the bottom of the air-plasma test cell and insulated from ground. The system is evacuated and pumped to approximately 1.5×10^{-7} Torr. The electron source is operated in a pulsed mode and the mesh voltage and graphite plate signal developed across load resistors are monitored as a function of electron source operating parameters: filament voltage and current. The graphite plate captures all the current flowing through the mesh and the optical pattern on the graphite plate confirms the beam is confined to a circular pattern on the plate.

The honeycomb and foil are installed. The mesh signal is then used to determine the beam current incident on the honeycomb and foil. The subsequent propagation of electrons through the foil into the test cell is modeled using a computational particle in cell code.

D. MAGIC Modeling.

A particle in cell simulation program from ATK Mission Research commonly called MAGIC was used to simulate the passage of electrons through the transmission window

foil and air in the test cell. The Appendix contains a chart of the modeling geometry and several representative plots of beam propagation at 10 Torr and 150 Torr as well as contour plots of beam current density as a function of depth into the test cell, see Appendix A-2. The results of this simulation effort appear in Fig. 8 for a 10-ma electron-beam current incident on the transmission window foil.

IONIZATION RATE AND BEAM CURRENT

RADIAL DISTRIBUTION

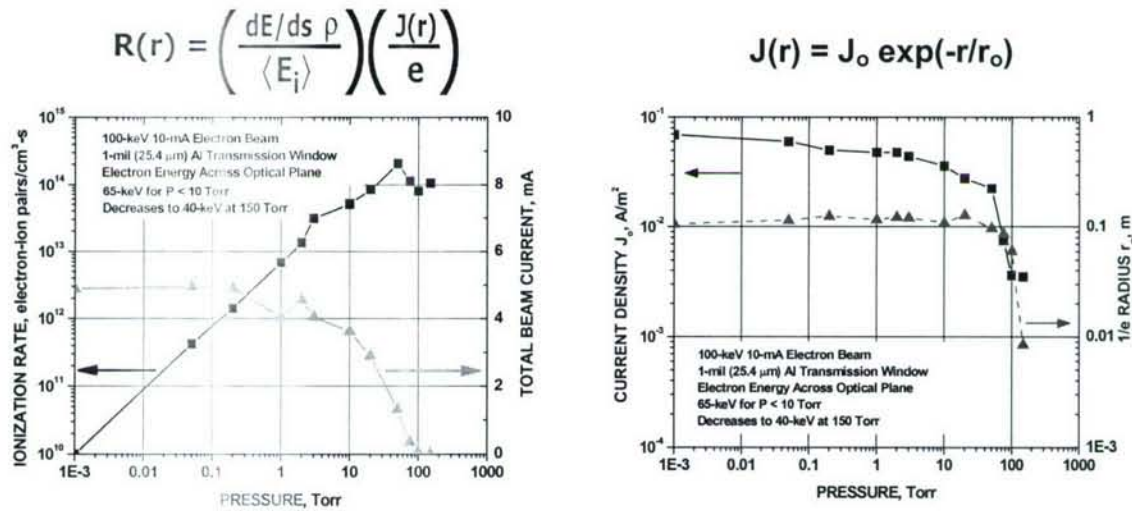


Figure 8. Mid plane ionization rate, beam current, and radial distribution.

The volumetric ionization rate in Fig. 8 represents the peak ionization rate for a radial distance $r = 0.0$ m. The formulas for the radial ionization rate $R(r)$, in electron-ion pairs per m^3 -s, and the radial current distribution $J(r)$ in A/m^2 appear in Fig. 8. The quantity dE/ds is the energy loss in aluminum in $J\text{-m}^2/\text{kg}$, ρ is the density of aluminum in kg/m^3 , $\langle E_i \rangle$ is the average energy to produce an electron-ion pair in air in J , e is the electron charge in C , J_0 is the maximum current density in A/m^2 , and r_0 is the $1/e$ radius of the current density in m . An exponential radial distribution was deduced from contour plots on the mid plane, such as the ones in the Appendix. The Gaussian electron-beam radial profile incident on the transmission window is transformed into non-Gaussian radial profile, because of electron scattering in the foil. At the mid plane of the test cell the contour-plot patterns in Appendix A have degraded to an extent that a Gaussian pattern is no longer present. An exponential profile is used instead.

E. RF Diagnostics.

A microwave absorption and phase measurement system was developed and installed in the air-plasma test cell within two large 8-inch CF nipples. The hardware to adapt the horns to the nipple is sketched in Fig. 9 and one of the nipples is shown in Figs. 3 and 4. Details of the absorption and phase measurement technique are in Vidmar *et al* (2006). The system operates at 10 GHz. Direct reflections from the curved cell wall proved to produce a strong reflection that adds to the direct (one-pass) signal

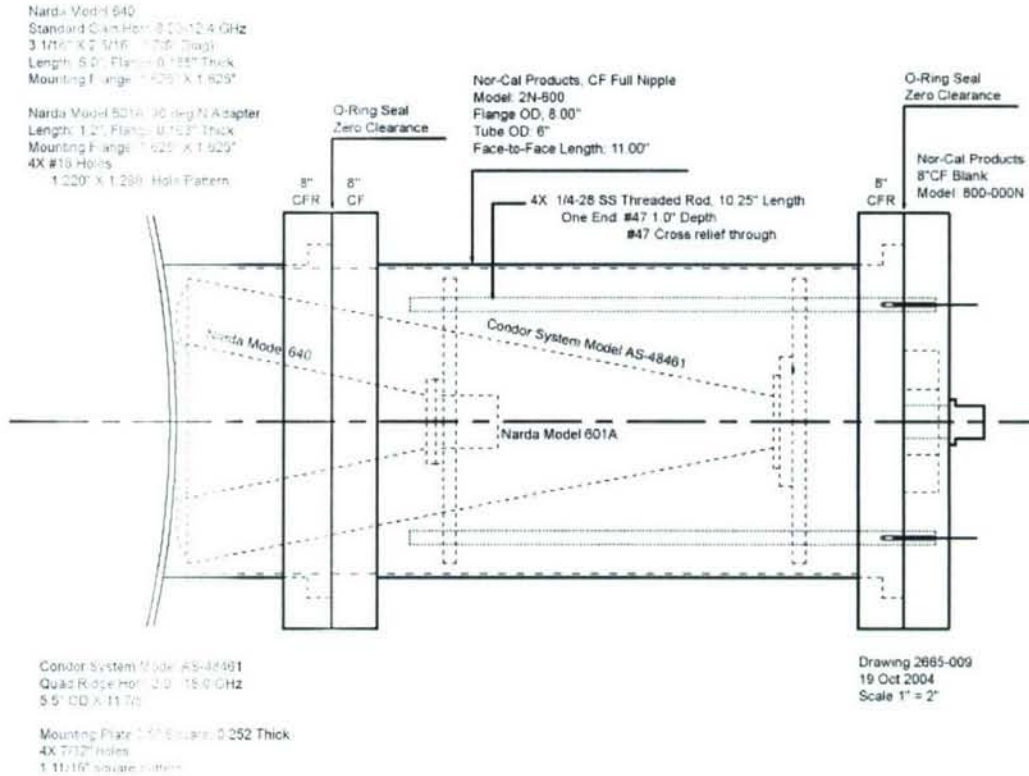


Figure 9. RF horn mounting fixture detail.

propagating through the test cell.

A 2-ft square panel of laminate absorber was used with a hole cut in the center for each of the 8-inch nipple and RF horn assemblies. The magnitude of signal reduction is evident in Fig. 10, as measured by a network analyzer operating in the time domain. The primary peak in Fig. 10 is the main signal propagating through the test cell. This peak has some structure that is due to minor reflections of cabling and connectors. The first peak 33.6 dB below the direct sign is due to reflection from the curved surface of the test cell covered with laminate absorber. The 33.6 dB signal is present in the phase detector along with the direct signal, which limits the phase resolution to approximately 1.2 deg.

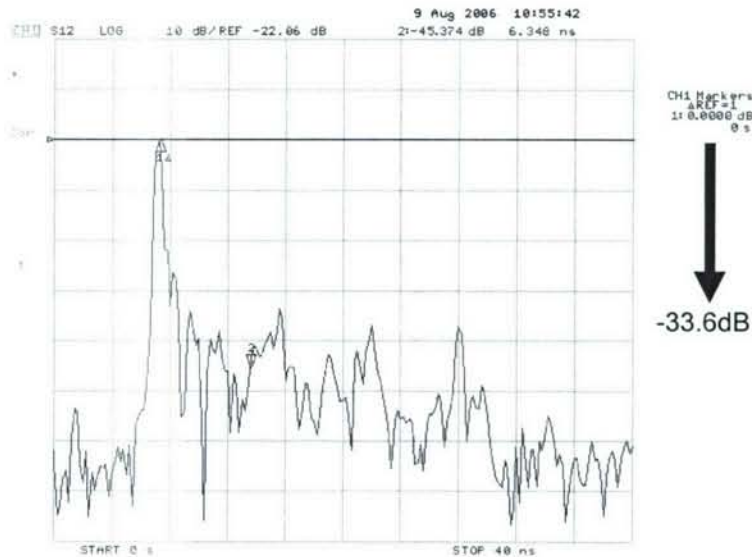


Figure 10. Time domain S_{12} of internal reflections at 10 GHz with absorber.

F. Ozone Detection.

The generation of ozone is a major byproduct of impact ionization of air with an electron beam. Its concentration and rate of increase provides data on the O concentration, because the theoretical production rates of O_3 depends on the O concentration. Measuring ozone is easier than measuring O directly. A White cell, as shown in Fig. 11, monitors the light passing through a 25 nm wide band-pass filter centered on 253.7 nm. This filter is close to the peak of ozone absorption. Figure 12 shows the detector and filter hardware details.

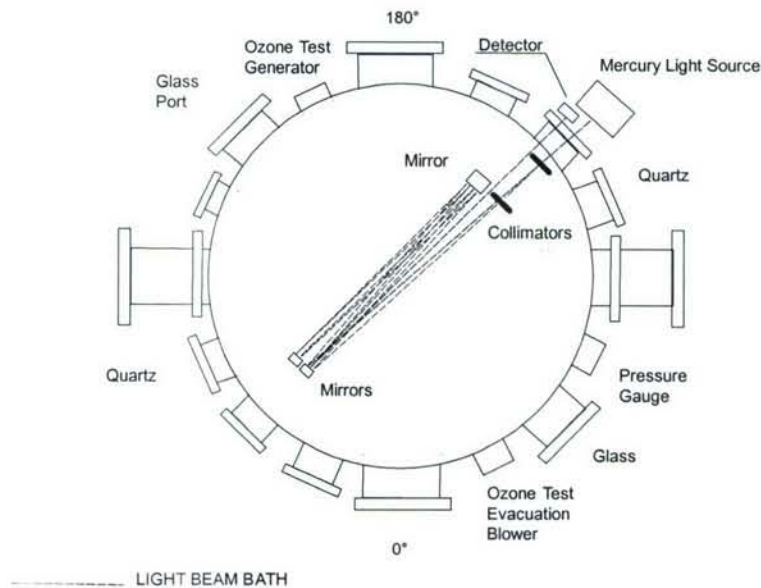


Figure 11. White cell mounted in air-plasma test cell for ozone measurement.

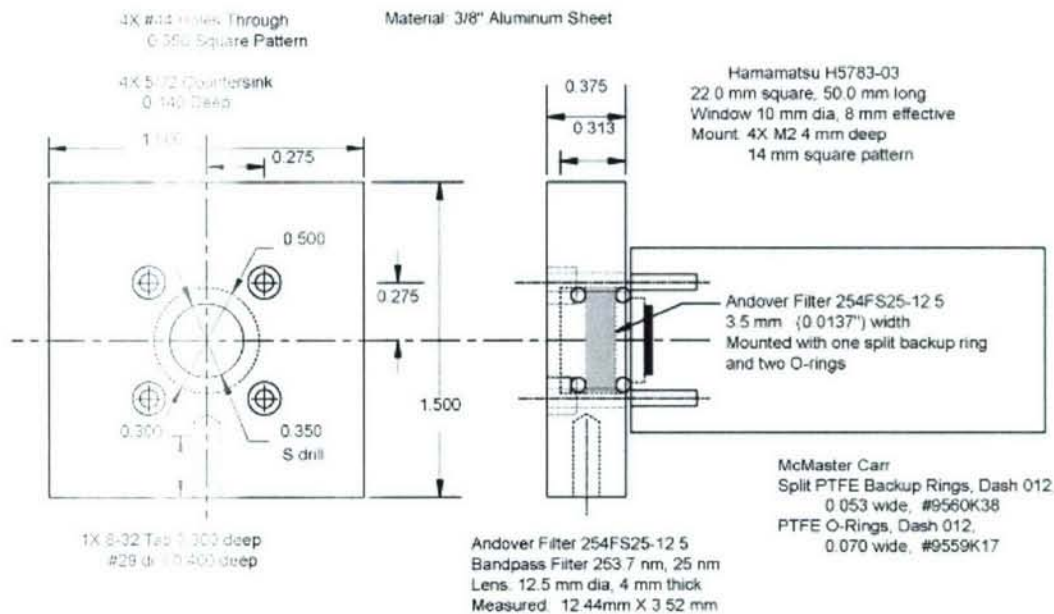


Figure 12. Hamamatsu H5783-03 fixture and filter housing.

G. Multichannel Simultaneous Data Acquisition.

The operation of the air-plasma test cell involves the simultaneous generation of an electron beam and monitoring sensors to record subsequent information as noted in Table 1. A short trigger pulse is used to simultaneously trigger two 4-channel digital sampling oscilloscopes that monitor the experiment for a few milliseconds. The mesh sensor voltage and transmission window signal quantify beam current and via MAGIC the ionization rate on the mid plane. The RF propagation path and optical signal paths cross the plasma on the mid plane of the test cell. The RF signals monitor both power absorption and 10 GHz phase from an I-Q detector. The ozone detector monitors light absorption and is used to quantify ozone production. In addition to these sensors, a spectrometer monitors optical emissions of nitrogen and will eventually provide real-time data.

Table 1 Multichannel diagnostics.

Channel 1	Trigger Pulse to Electron Gun
2	Mesh Voltage to Monitor Beam Current
3	Transmission Window Foil
4	RF Power Absorption
5	RF I-Channel Phase
6	RF Q-Channel Phase
7	Ozone Signal

III RESULTS

The major research results are the following:

- An experimental test facility consisting of a 100-keV electron gun and a 400-liter air-plasma test cell with microwave, optical, and electronic diagnostics has been developed for studies of air-plasma generation at pressures from 1 mTorr to 760 Torr.
- Preliminary measurements have been made with all sensors and improvements to the infrastructure associated with reliable electron source operation are progressing.

IV PERSONNEL, INTERACTIONS, AND PUBLICATIONS

1 Dec 2003 – 31 May 2007

Personnel. The primary personnel on this project has been

- Robert J Vidmar, Principal Investigator
- Kenneth R Stalder, Consultant

Interactions. The research conducted on this project has been presented at the 57th, 58th, and 59th Gaseous Electronic Conferences, and at the 42nd, 43rd and 44th Aerospace Sciences Meeting and Exhibit American Institute of Aeronautics and Astronautics Conference in Reno Nevada, 31st and 33rd International Conference on Plasma Science, and the 2007 Pulsed Power and Plasma Science Conference. There were numerous interactions at these conferences with representatives from DoD Laboratories, National Laboratories, private companies, and Universities from around the world.

Publications Supported by AFOSR Grant Number FA9550-1-0015

- Vidmar, R. J., and K. R. Stalder, "Electron-Beam Generated Plasma in Air: Pulsed and Continuous Generation," Session 51-WIG-2, AIAA 2004-0359, p 8, 42nd Aerospace Sciences Meeting and Exhibit, Reno, NV, 5-8 Jan, 2004.
- Vidmar, R. J., "High-Pressure Liquid Cooling for High Repetition-Rate Capacitors," 31st IEEE International Conference on Plasma Science, 28 June -1 July, 2004, Baltimore, MD.
- Vidmar, R. J., "High Repetition-Rate Liquid Cooled Capacitors," 31st IEEE International Conference on Plasma Science, 28 June -1 July, 2004, Baltimore, MD.
- Stalder, K, Vidmar, R., Nersisyan, G., and W. Graham, "Modeling the Kinetics in High-Pressure Glow Discharges," PT2.059, 57th Annual Gaseous Electronics Conference, 26-29 Sept, Shannon, The Republic of Ireland, GEC04, 2004, Bulletin of the American Physical Society, 2004.
- Vidmar, R. J., and K. R. Stalder, "Air-Plasma Experimentation at the University of Nevada, Reno," Session 111-WIG-5, AIAA 2005-0791, p 12, 43rd Aerospace Sciences Meeting and Exhibit, Reno, NV, 10-13 Jan, 2005.
- Vidmar, R., K. Stalder, and M. Seeley, "Air-Plasma Test Cell, Electron-Beam Source, and Measurements of Electron Density and Ozone Concentration," DM1-6, 58th Annual Gaseous Electronics Conference, 16-20 Oct 2005, San Jose, CA, GEC05, 2005, Bulletin of the American Physical Society, Vol 50, No 7, p 16, 2005.
- Vidmar, R., K. Stalder, and M. Seeley, "Experimental Details on Air-Plasma Measurements of Electron Density and Ozone Concentration," SW33, 58th Annual Gaseous Electronics Conference, 16-20 Oct 2005, San Jose, CA, GEC05, 2005, Bulletin of the American Physical Society, Vol 50, No 7, p 55, 2005.

- Vidmar, R., K. Stalder, and M. Seeley, "Electron Beam Produced Air Plasma: Measurements of Electron Density and Ozone Concentration," Session 116-WIG-4, AIAA 2006-0791, p 10, 44th Aerospace Sciences Meeting and Exhibit, Reno, NV, 9-12 Jan, 2006.
- Vidmar, R., K. Stalder, and M. Seeley, "Electron-Beam Produced Air Plasma: Optical Measurements of Beam Current," Oral Presentation LW1-7, 59th Annual Gaseous Electronics Conference, 10-13 Oct 2006, Columbus, OH, GEC06, 2006, Bulletin of the American Physical Society, Vol 51, No 5, p 41, ISSN 0003-0503(200610)51;5;1-S, 2006.
- Vidmar, R., K. Stalder, and M. Seeley, "Electron-Beam Produced Air Plasma: Optical and Electrical Diagnostics," Poster SRP2-13, 59th Annual Gaseous Electronics Conference, 10-13 Oct 2006, Columbus, OH, GEC06, 2006, Bulletin of the American Physical Society, Vol 51, No 5, p 41, ISSN 0003-0503(200610)51;5;1-S, 2006.
- Stalder, K. R., R. J. Vidmar, G. Nersisyan, and W. G. Graham, "Modeling the Chemical Kinetics of High-Pressure Glow Discharges in Mixtures of Helium with Real Air," Journal of Applied Physics, Vol 99, No 9, pp 93301-1-8, 1 May 2006.
- Vidmar, R.J., K.R. Stalder, and M.V. Seeley, "Electron-Beam Produced Air Plasma: RF and Optical Diagnostics," 33rd IEEE International Conference on Plasma Science, 4-8 June 2006, Traverse City, Michigan, Poster 1P35, p 156, IEEE 06CH37759, ISBN 1-4244-0124-0, June 2006.
- Vidmar, R.J., K.R. Stalder, and M.V. Seeley, "Electron-Beam Produced Air Plasma: Optical and Electrical Observations," 33rd IEEE International Conference on Plasma Science, 4-8 June 2006, Traverse City, Michigan, Oral Presentation 3D6, p 219, IEEE 06CH37759, ISBN 1-4244-0124-0, June 2006.
- Serdyuchenko, A. Y., M. V. Seeley, Q. J. Sinnott, and R. J. Vidmar, "Application of Tunable Diode Laser Spectroscopy for Time Resolved Measurements in Electron Beam Produced Plasma," 2007 IEEE Pulsed Power and Plasma Science Conference, 17-22 June 2007, Albuquerque, New Mexico, Poster 2P10, June 2007.
- Vidmar, R.J., A. Y. Serdyuchenko, M. V. Seeley, Q. J. Sinnott, and K. R. Stalder, "Electron-Beam Generated Air Plasma: Sensors to Quantify Beam Current and Electron Density," 2007 IEEE Pulsed Power and Plasma Science Conference, 17-22 June 2007, Albuquerque, New Mexico, Poster 2P26, June 2007.
- Serdyuchenko, A. Y., M. V. Seeley, Q. J. Sinnott, and R. J. Vidmar, "Chemical Composition of Electron Beam Produced Air Plasma by Means of Tunable Diode Laser Spectroscopy and Numerical Simulation," 2007 IEEE Pulsed Power and Plasma Science Conference, 17-22 June 2007, Albuquerque, New Mexico, Oral Presentation 3F1, June 2007.
- Vidmar, R.J., A. Y. Serdyuchenko, M. V. Seeley, Q. J. Sinnott, and K. R. Stalder, "Electron-Beam Generated Air Plasma: Beam Current and Electron Density Distributions," 2007 IEEE Pulsed Power and Plasma Science Conference, 17-22 June 2007, Albuquerque, New Mexico, Oral Presentation 3B7, June 2007.

REFERENCES

- Adamovich, I. V., "Control of Electron Recombination Rate and Electron Density in Optically-Pumped Non-Equilibrium Plasmas," *J. Phys D: Appl. Phys.*, Vol 34, No 3, pp 319-325, 7 Feb, 2001.
- Macheret, S. O., M. N. Shneider, and R. B. Miles, "Modeling of Discharges Generated by Electron Beams in Dense Gases: Fountain and Thunderstorm Regimes," *Physics of Plasmas*, Vol 8, No 5, pp 1518-1528, May, 2001.
- Stark, R. H., and K Schoenbach, "Electron Heating in Atmospheric Pressure Glow Discharges," *J. Appl. Phys.*, Vol. 89, No. 7, pp 3568-3572, 1 April 2001.
- Vidmar, R. J., Plasma Cloaking: Air Chemistry, Broadband Absorption, and Plasma Generation, NTIS, AFOSRTR900544, ADA2220440, p 88, 1990A.
- Vidmar, R. J., "On the Use of Atmospheric Pressure Plasmas as Electromagnetic Reflectors and Absorbers," *IEEE Transactions on Plasma Science*, Vol 18, No 4, pp 733-741, Aug, 1990B.
- Vidmar, R., K. Stalder, and M. Seeley, "Electron Beam Produced Air Plasma: Measurements of Electron Density and Ozone Concentration," Session 116-WIG-4, AIAA 2006-0791, p 10, 44th Aerospace Sciences Meeting and Exhibit, Reno, NV, 9-12 Jan, 2006.
- Yu, L, C. O. Laux, DM Packan, and C. H. Kruger, "Direct-Current Glow Discharges in Atmospheric Pressure Air Plasma," *J. Appl. Phys.*, Vol. 91, No. 5, pp 2678-2686, 1 March 2002.

APPENDIX

MAGIC TEST CELL GEOMETRY	A-2
MAGIC DIAGNOSTIC DATA	A-3

FIGURES

Figure A1. Geometry of air-plasma test cell used for MAGIC modeling.	A-2
Figure A2. Propagation in 10 Torr air.	A-3
Figure A3. Propagation in 150 Torr air.	A-3
Figure A4. Electron beam current density incident on transmission-window foil.	A-4
Figure A5. Electron beam current density on plane $z = 10.51$ cm.	A-4
Figure A6. Electron beam current density on mid plane $z = 30.56$ cm.	A-5
Figure A7. Electron-beam energy versus distance at 10 Torr.	A-6
Figure A8. Electron-beam current versus distance at 10 Torr.	A-6

MAGIC TEST CELL GEOMETRY

The air-plasma test cell and electron beam transmission window were modeled in Cartesian coordinates. The side view in Fig. A1 is a two dimensional, y-z plot for $x = 0$ cm. The electron beam enters a vacuum section 6 cm in diameter at $z = 0$ cm. A Teflon insulator supports an aluminum clamping ring connected to ground via a load resistor. The transmission window is at $z = 5$ cm. The mid plane is half way into the tank and has $z = 30.5$ cm (12 inch).

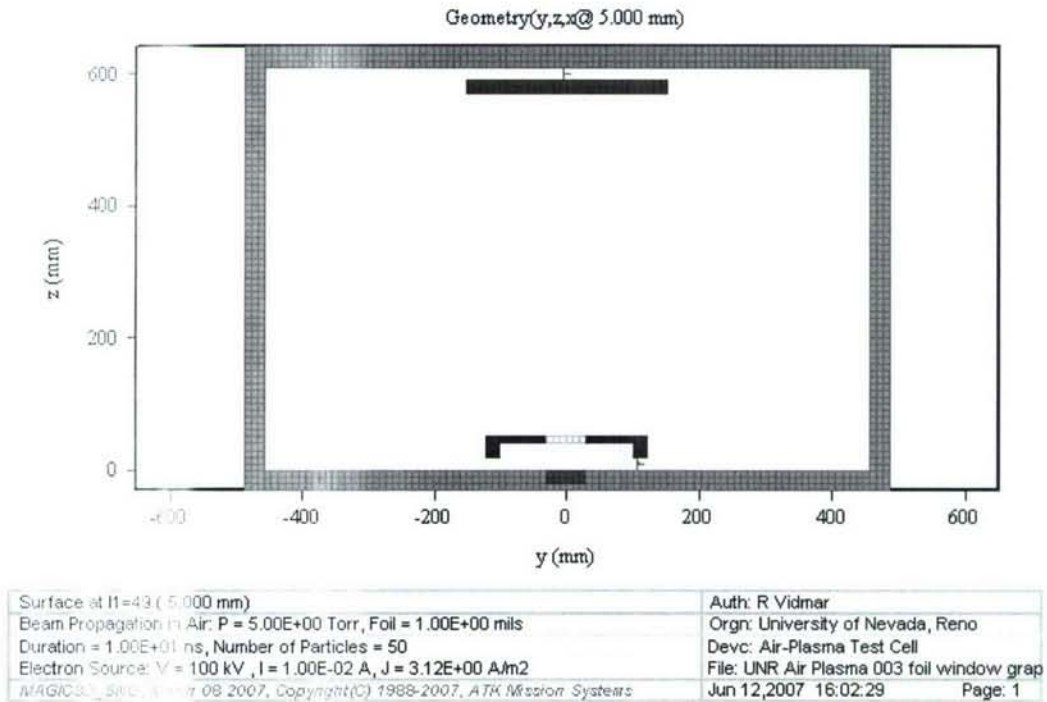


Figure A1. Geometry of air-plasma test cell used for MAGIC modeling.

MAGIC DIAGNOSTIC DATA

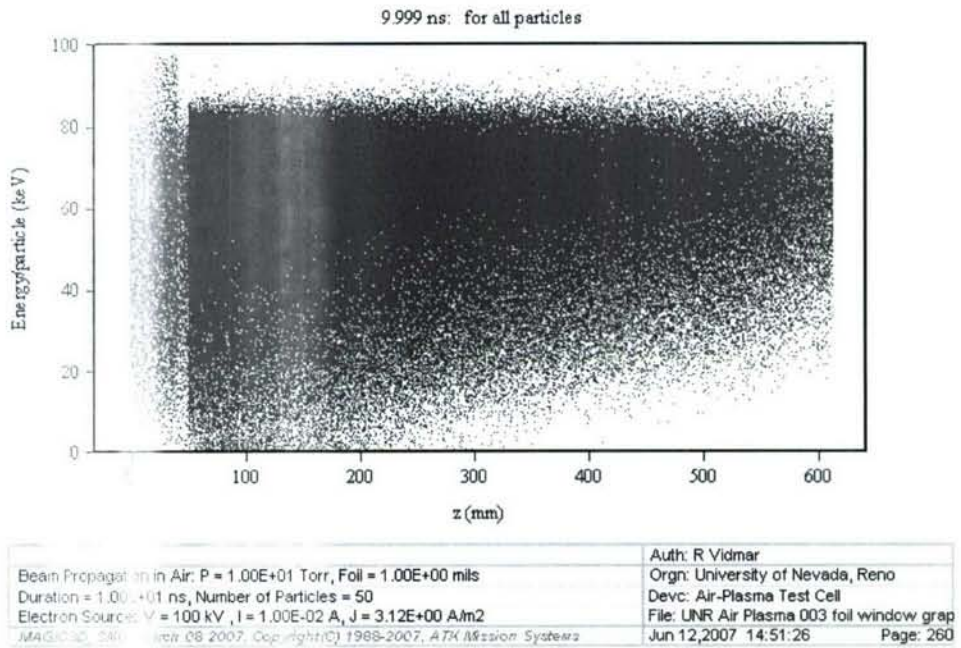


Figure A2. Propagation in 10 Torr air.

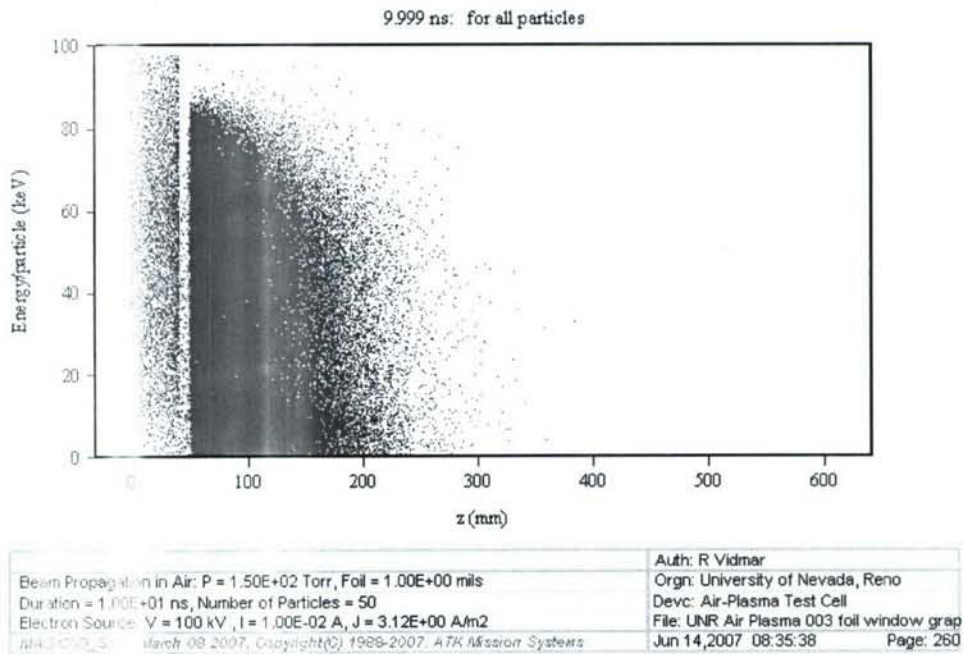


Figure A3. Propagation in 150 Torr air.

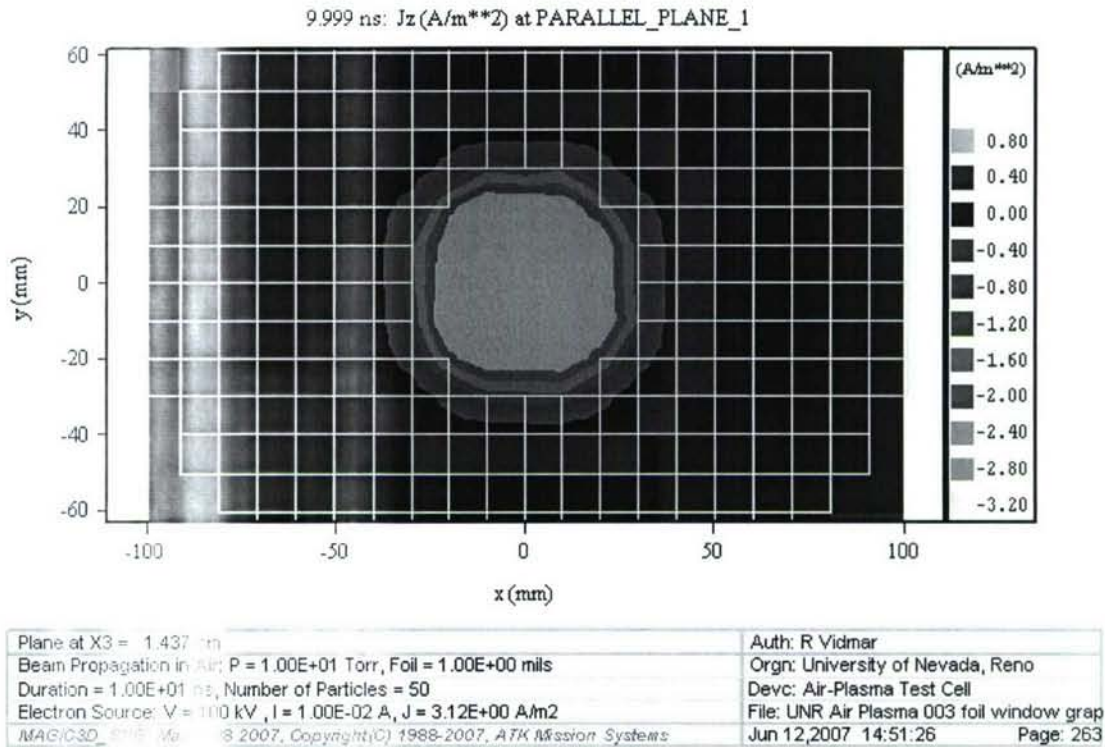


Figure A4. Electron beam current density incident on transmission-window foil.

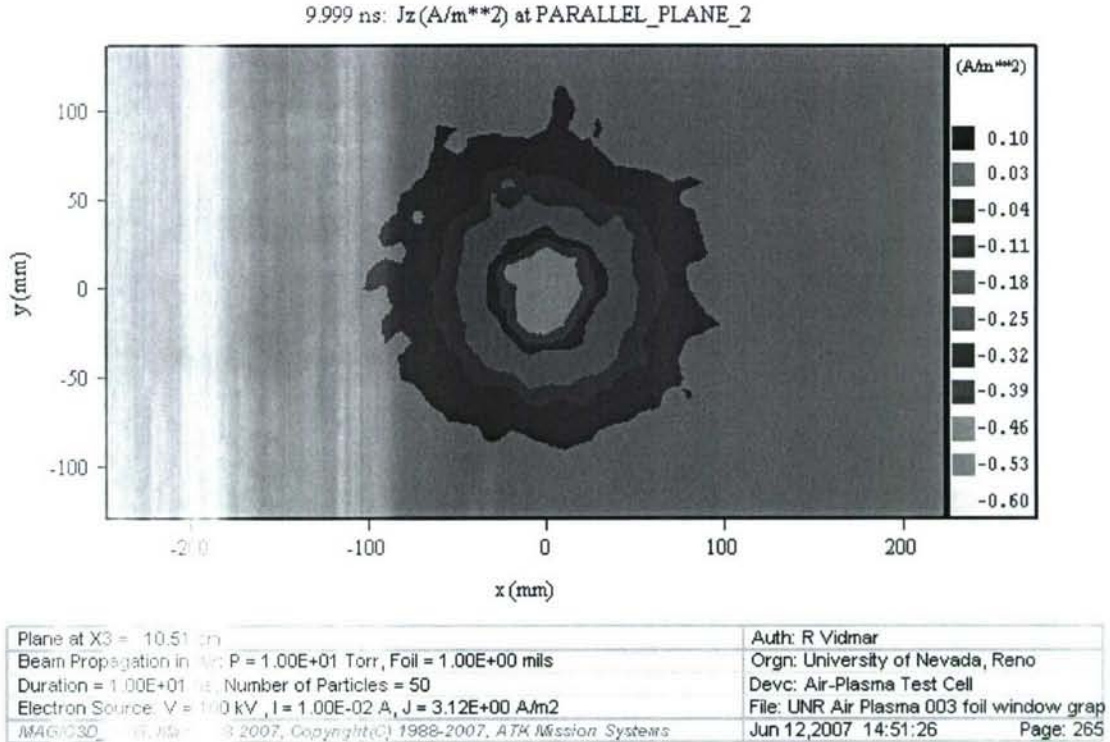
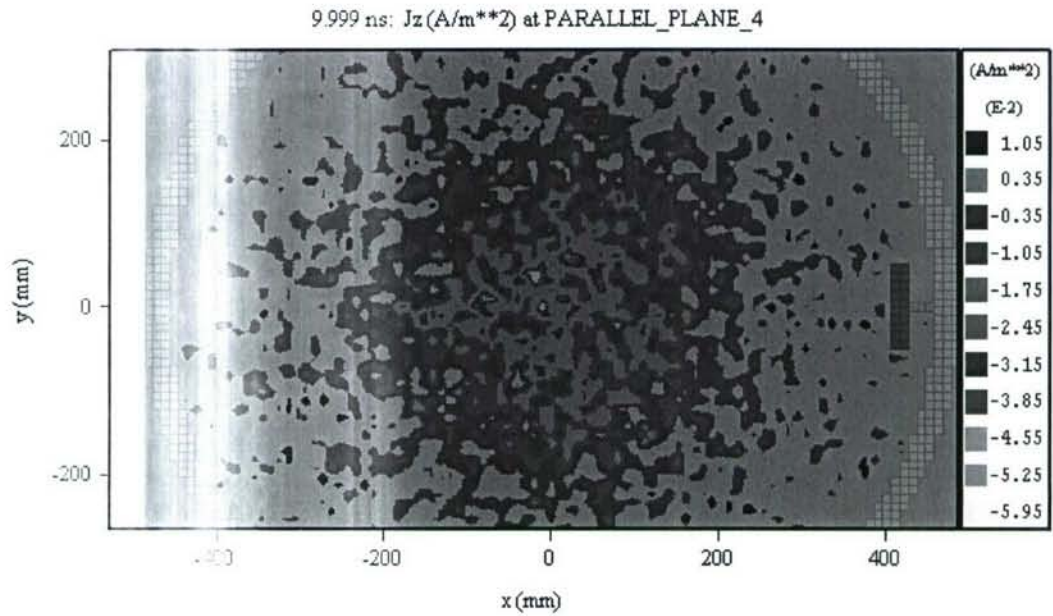


Figure A5. Electron beam current density on plane z = 10.51 cm.



Surface at I3=34 (30.56 cm)	Auth: R Vidmar
Beam Propagation in Air: P = 1.00E+01 Torr, Foil = 1.00E+00 mils	Orgn: University of Nevada, Reno
Duration = 1.00E+01 ns, Number of Particles = 50	Devc: Air-Plasma Test Cell
Electron Source: V = 100 kV, I = 1.00E-02 A, J = 3.12E+00 A/m2	File: UNR Air Plasma 003 foil window grap
MAGIC-3D, Sims, R. 2007, Copyright(C) 1988-2007, ATK Mission Systems	Jun 12, 2007 14:51:26 Page: 267

Figure A6. Electron beam current density on mid plane $z = 30.56$ cm.

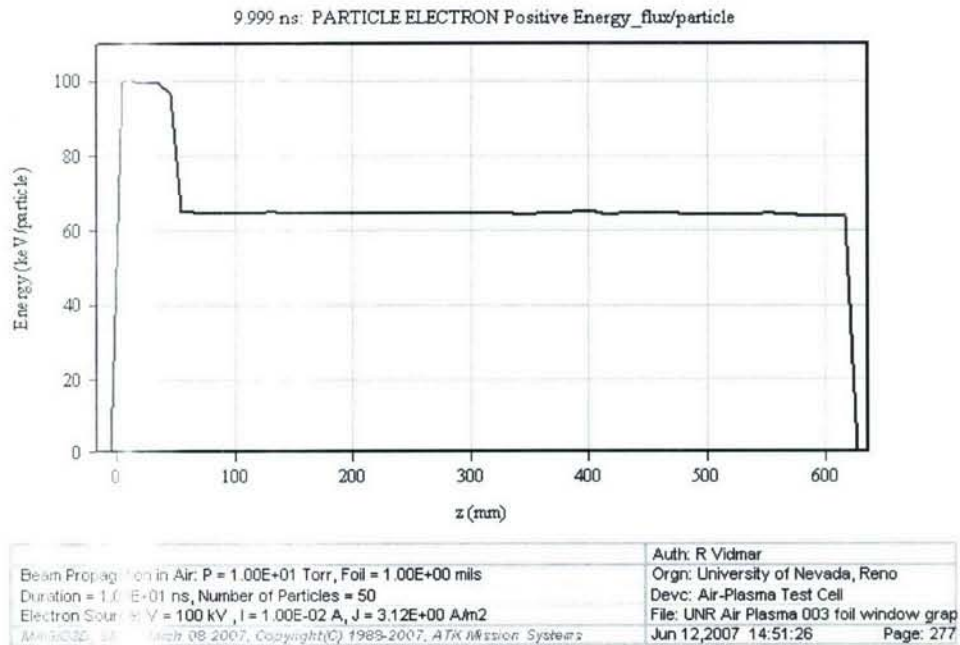


Figure A7. Electron-beam energy versus distance at 10 Torr.

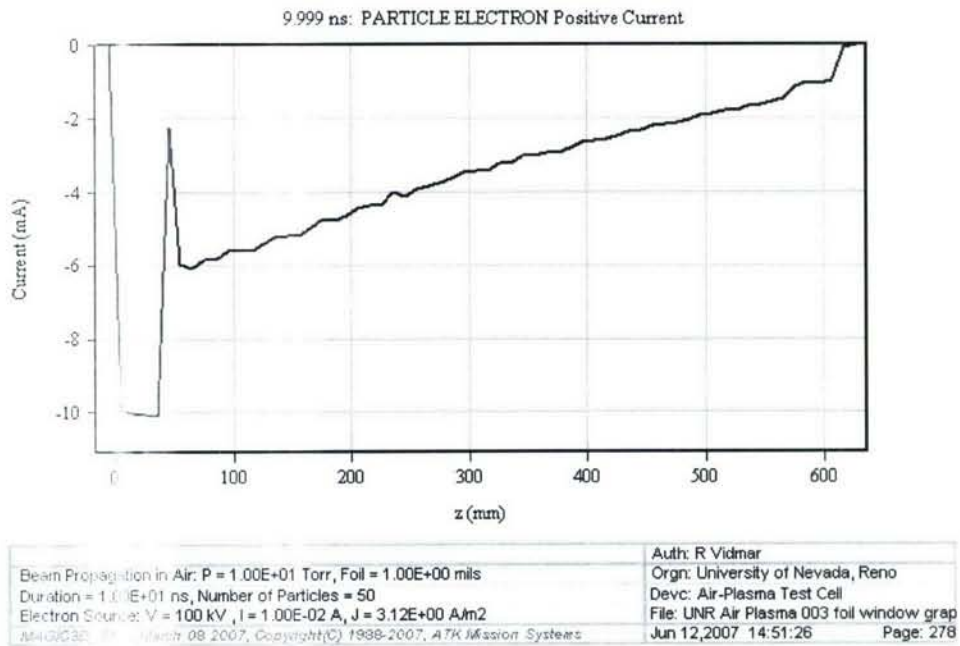


Figure A8. Electron-beam current versus distance at 10 Torr.